

Laser & Optoelectronics Progress

Carrier-Envelope Phase-Dependent Phase Matching of Terahertz Emission in Laser Plasma

Wang Shuo^{1,2}, Li Fangshu^{1,3}, Lu Haocheng^{1,2}, Zheng Wenyang^{1,2}, Zhao Xulin^{1,4}, Jiang Yang^{1,2},
Li Na^{1,5*}, Bai Ya^{1,2**}, Liu Peng^{1,2}

¹State Key Laboratory of High Field Laser Physics and CAS Center for Excellence in Ultra-Intense Laser Science, Shanghai Institute of Optics and Fine Mechanics, Chinese Academy of Sciences, Shanghai 201800, China;

²Center of Materials Science and Optoelectronics Engineering, University of Chinese Academy of Sciences, Beijing 100049, China;

³China MOE Key Laboratory of Advanced Micro-Structured Materials, Institute of Precision Optical Engineering, School of Physics Science and Engineering, Tongji University, Shanghai 200092, China;

⁴Department of Physics, Shanghai University, Shanghai 200444, China;

⁵School of Physics and Electronic Engineering, Xinxiang University, Xinxiang 453003, Henan, China

Abstract We investigate off-axis phase-matched terahertz (THz) radiation in laser plasma pumped by few-cycle laser pulses. We find that the THz amplitude and angular distributions in the far field are sensitively dependent on the pump pulse's focal carrier-envelope phase (CEP). Ring-like profiles of THz radiation are obtained at CEP values of 0.5π and 1.5π , due to the inversely symmetric local THz waveforms emitted before and after laser focus. Off-axis phase-matched THz radiation offers a tool to accurately measure the CEP of few-cycle pulses at the center of a medium.

Key words terahertz radiation; carrier-envelope phase; laser plasma; off-axis phase-matching

中图分类号 O437.5

文献标志码 A

DOI: 10.3788/LOP230448

1 Introduction

Ultrashort laser pulses are a powerful tool for probing electronic dynamics in the attosecond regime. The carrier-envelope phase (CEP) of ultrashort laser pulses defines the phase of carrier wave at the instant of maximum amplitude of the pulse envelope. As the pulse duration is comparable to the oscillation cycle of the carrier wave, the CEP becomes a critical parameter, whose variation will significantly modify the laser field and the nonlinear interaction with gaseous or condensed media^[1-3]. Over the last decade, investigations on CEP-dependent phenomena have been continuously conducted. Accurate CEP measurement has become a challenging goal in manipulating physical mechanisms with a laser field. Methods such as high-order harmonics generation^[4-5], stereo above-threshold

ionization (stereo-ATI)^[6-8], terahertz (THz) emission^[9-14], and Compton scattering^[15] have been developed to measure the CEP of few-cycle pulses. Unlike the stereo-ATI method, which measures the ATI electrons in high vacuum, CEP measurement using THz emission from laser plasma is convenient. However, these methods suffer from variations caused by the Gouy phase shift of the Gaussian beam and phase shifts triggered by the nonlinear interaction of intense pulses with the medium^[10, 16].

By focusing few-cycle pulses in ambient air, transient photocurrents are produced from laser-induced plasma to generate enhanced THz radiation, whose waveform is sensitive to the CEP^[9, 10, 12, 17]. As the laser pulse propagates, the Gouy phase shift and diffraction dominate the CEP variation^[16]. The phase variation can be as large as π for a focused Gaussian beam^[18]. As a

收稿日期: 2023-01-05; 修回日期: 2023-01-05; 录用日期: 2023-01-06; 网络首发日期: 2023-01-16

基金项目: 国家自然科学基金 (11874373, 2174412)、中国科学院科研仪器设备研制项目 (YJKYYQ20180023)、河南省自然科学基金 (202300410017)、新乡学院博士科研启动项目 (1366020150)

通信作者: *lina2011@siom.ac.cn; **pipbear@siom.ac.cn

result, it is not easy to determine the precise value of the CEP in the interaction region, whereas only the modulation of experimental observations is measured by varying the CEP. THz waveforms inside the laser plasma show a characteristic evolution that depends on the CEP of few-cycle pulses before focusing, therefore, the concept of an initial CEP was proposed to accurately define the phase of the pump pulses. However, this phase is not the CEP in the interaction region^[12].

This study investigates the phase-matching condition of THz radiation from a few-cycle pulse-pumped laser plasma. It was observed that the spatial distribution of the off-axis THz emission is dependent on the CEP value at the center of the laser focus. In particular, the far-field profile of THz emission exhibits a ring-like pattern with a central dark spot for the driven pulse's CEP of 0.5π and 1.5π . Such features persist even when the interaction region extends to the entire Rayleigh length. This finding offers a means of accurately measuring the CEP of few-cycle pulses at the center of the medium, which is crucial for understanding the underlying physics of CEP-related phenomena.

2 Methods

The far-field THz intensity distribution produced by few-cycle pulses can be obtained by the coherent superposition of local THz radiation from the air plasma. We evaluated the THz profile based on the propagation of the local THz emission from the laser-induced photocurrent. Considering the finite lifetime of free electrons in laser plasma, the local THz radiation^[19-21] is given by

$$\frac{\partial J_e(t)}{\partial t} + \frac{J_e}{\tau_e} = \frac{E_L(t)q_e^2}{m_e} \rho_e(t), \quad (1)$$

$$\frac{d\rho_e(t)}{dt} = W_{\text{ADK}}(t)[\rho_{\text{at}} - \rho_e(t)], \quad (2)$$

$$E_{\text{THz}}(t) \propto \frac{\partial J_e(t)}{\partial t}, \quad (3)$$

where J_e is the photocurrent, τ_e is the free-electron lifetime^[22], m_e is the electron mass, q_e is the electron charge, ρ_e is the electron density, and ρ_{at} is the molecular density of ambient air. Here, W_{ADK} is the ionization rate and was calculated based on ADK theory^[23] as follows

$$W_{\text{ADK}}(t) = \omega_p |C_{n^*}|^2 \left(\frac{4\omega_p}{\omega_l} \right)^{2n^*-1} \exp\left(-\frac{4\omega_p}{3\omega_l} \right), \quad (4)$$

$$\omega_p = \frac{I_p}{\hbar}, \quad (5)$$

$$\omega_l = \frac{eE_L(t)}{(2mI_p)^{\frac{1}{2}}}, \quad (6)$$

$$n^* = Z \left(\frac{I_{\text{ph}}}{I_p} \right)^{\frac{1}{2}}, \quad (7)$$

$$|C_{n^*}|^2 = 2^{2n^*} [n^* \Gamma(n^* + 1) \Gamma(n^*)]^{-1}, \quad (8)$$

where I_p is the ionization potential of the gaseous medium, I_{ph} is the ionization potential of the hydrogen atom, and $E_L(t)$ is the laser field. The far field THz emission^[24] is then calculated in the frequency domain as

$$\tilde{E}_F(x, y, \Omega) \propto \sum_{j=1}^V \tilde{E}_{\text{THz}}(j) \frac{\exp[ik_{\text{THz}}R(j)]}{R(j)} \exp[in_g k_{\text{THz}}z(j)], \quad (9)$$

where V is the interaction range, R is the distance between the interaction point and a point on the detection screen, n_g is the pump field's group-velocity index of refraction in the medium (in a weakly ionized medium, $n_g \approx 1$), and z is the propagation axes coordinate. The laser focus is set at $z = 0$.

The laser field of $E_L(z, r, t)$ is written as a Gaussian beam as follows:

$$E_L(z, r, t) = E_0 \frac{\omega_0}{\omega_z} \exp\left(-\frac{r^2}{\omega_z^2} - \frac{t^2}{g^2} \right) \exp\left[\frac{ikr^2z}{2(z^2 + z_R^2)} \right] \exp\left[-i \arctan\left(\frac{z}{z_R} \right) \right] \exp[i(kz - \omega t + \varphi_0)], \quad (10)$$

Where E_0 is the peak intensity, ω_0 is the beam waist, ω_z is the beam radius, g is the pulse envelope parameter, z_R is the Rayleigh length, $-i \arctan(z/z_R)$ is the Gouy phase shift, and φ_0 is the CEP value at the center of the laser focus. The CEP evolution of few-cycle laser pulses propagated in the laser plasma can be modified by the Kerr effect and plasma-induced dispersion^[10]. In a weakly ionized medium caused by a low-energy few-cycle pulse, the Kerr effect and plasma-induced dispersion only change the value of CEP slightly but do not influence the asymmetric distribution feature of the CEP along the medium, so these two terms can be neglected in this scheme. Therefore, the CEP of the propagating laser pulse is dependent on both the Gouy phase shift and φ_0 , which will be changed by π over the laser-focusing region. In the simulation, the wavelength of the pump pulse was $0.8 \mu\text{m}$, the full width at half maximum (FWHM) of the laser pulses was 6 fs (~ 2.2 cycles), $\omega_0 = 50 \mu\text{m}$, and the peak intensity was $1 \times 10^{14} \text{ W/cm}^2$. Argon (Ar) gas was

used as the medium at standard atmospheric pressure, and the detection screen was placed 300 mm away from the focal point.

3 Results and Discussions

Figures 1 (a) and 1 (b) show the local THz waveforms inside the plasma for the focal CEP, $\varphi_0 = 0.5\pi, 0.6\pi$, respectively. As shown in Fig. 1(a), the THz emission gradually changes its amplitude and polarity when coordinate z is varied, and at the center position, the THz emission signal weakens and then reverses the polarity. Fig 1 (b) shows that the waveform becomes more symmetric at approximately 0 ps, whereas the THz wave almost maintains its polarity for $\varphi_0 = 0.6\pi$. In both cases, the local THz intensity drops rapidly outside the laser focus owing to the rapidly decreasing pump pulse intensity. In Fig. 1(c), we plotted the on-axis ($x, y = 0$) temporal waveforms of the local THz emission for $\varphi_0 = 0.5\pi$ at $z = -3$ mm (black curve) and 3 mm (red curve). The polarity

reversal of the THz field occurs because of the change in the CEP caused by the Gouy phase shift. Figure 1(d) shows the amplitude of the local THz radiation along the propagation axis with the CEP of 0.5π (solid curve) and 0.6π (dashed curve) at the focus, with amplitudes below and above zero representing negative and positive THz wave polarity, respectively. Figure 1(d) also shows the variation in the pulse CEP with different values of φ_0 in the dashed yellow curve, which represents an asymmetric distribution feature because of the Gouy phase shift. The above discussions indicate that the evolution of local THz waveforms is sensitive to φ_0 . Furthermore, the change in THz waveform polarity was calculated with φ_0 varying from 2π to 0, as shown in Fig. 1(e). It should be noted that $\varphi_0 = 0.5\pi$, and 1.5π are special cases in which the THz waveforms are inversely symmetric at the same distance before and after the laser focus. This explains the symmetric THz amplitude shown in Fig. 1(d) (green curve).

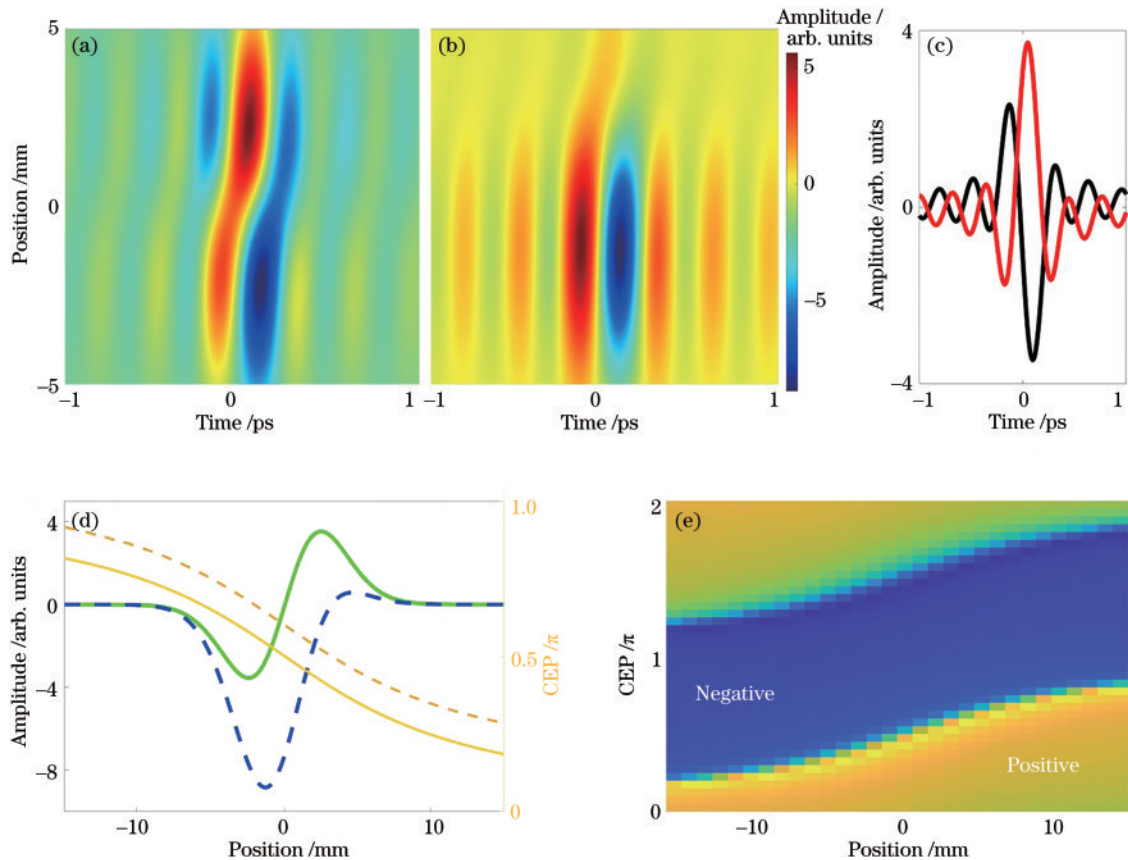


Fig. 1 Local THz generated at different positions of medium. THz waveform evolved with position with different φ_0 of (a) 0.5π and (b) 0.6π ; (c) THz waveforms from different position -3 mm (black curve) and 3 mm (red curve) in Fig. 1(a); (d) THz amplitude taken from Fig. 1(a) (green solid curve) and Fig. 1(b) (blue dash curve) at the time of 0 ps and pulse CEP shown in yellow solid curve ($\varphi_0 = 0.5\pi$) and yellow dash curve ($\varphi_0 = 0.6\pi$); (e) polarity of local THz

The far-field distribution directly depends on the local THz source inside the plasma. As an example,

THz waves generated with the same amplitude and opposite polarity will cancel out in the forward

direction, whereas they constructively interfere in a specific off-axis direction ($\sim 7^\circ$). In this case, the THz waves will have a half wavelength path difference given by $[|AP| - (|AB| + |BP|)] = \Gamma/2$, where Γ is the wavelength of THz emission], as illustrated in Fig. 2. In other words, along with the laser plasma, antisymmetric THz emission can produce phase-matched ring-like radiation, as shown in Fig. 1 (d) (green solid curve).

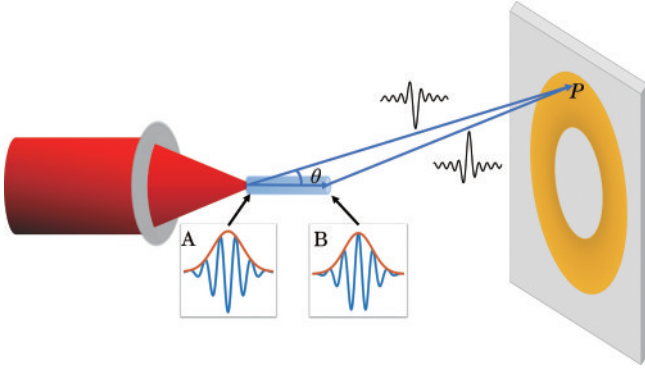


Fig. 2 Schematic diagram of off-axis phase matching

The far-field distributions calculated using Eq. (9) for $\varphi_0 = 0.5\pi, 0.6\pi$ and the plots are shown in Fig. 3(a) and (b), respectively. A ring-like profile is displayed for $\varphi_0 = 0.5\pi$, but a round spot with a near-flat top profile is obtained for 0.6π . The profile in Fig. 3(a) is similar to that reported in Ref. [24-25], in which the pump pulse is a two-color laser field. The hollow-core THz radiation pattern is also caused by the off-axis phase-matching condition created by the reversed local THz polarity due to the dephasing of the two-color laser field. In addition, a ring-shaped THz profile can be produced for $\varphi_0 = 1.5\pi$ (for 1.5π , the results are identical with those for 0.5π). Under experimental conditions^[26-27], THz can radiate from a short dimension of less than 2 mm in vacuum. We calculated the THz emission from much shorter medium lengths of 6 mm and 2 mm with $\varphi_0 = 0.5\pi$, which are shown in Fig. 3(c) and Fig. 3(d), respectively. Clearly, the patterns in both cases show different phase-matching angles and sharpness but maintain a ring-shaped profile.

The far-field distribution of different THz frequencies directly determined the accuracy in identifying the ring-like pattern because of the broad spectrum of THz emission. To clarify these details, the angular distributions at different THz frequencies were calculated with $\varphi_0 = 0.5\pi$, as shown in Fig. 4. The phase-matching angle (θ) tends to decrease with increasing THz frequency^[24]. The angle (θ) can be well predicted by $\cos(\theta) = 1 -$

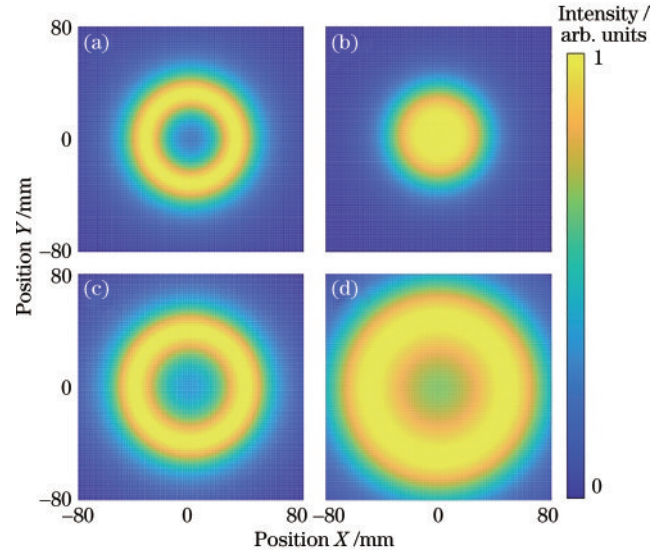


Fig. 3 THz far-field intensity distribution (< 3 THz) with different φ_0 of (a) 0.5π and (b) 0.6π ; different medium length (c) 6 mm and (d) 2 mm

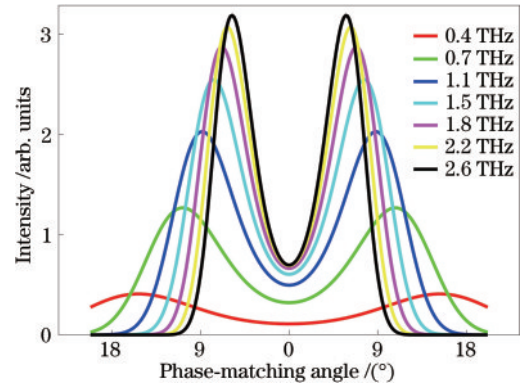


Fig. 4 Phase-matching angle with different THz frequencies

$\Gamma/2l_d$, where l_d is the half-length of the local THz generation range and is 10 mm in this scheme. This frequency-dependent angular distribution feature indicates coherent interference, in which phase matching occurs in the off-axis direction. The radiation attained at all frequencies superimpose to produce ring-like radiation.

For a measured THz profile in the far field, the CEP can be distinguished by finding the maximum value in the profile divided by the minimum value in the center area. The peak-to-valley ratio of the far-field profile with varying center CEP values is shown in Fig. 5. The two peaks at 0.5π and 1.5π represent two standout ring-like distributions, as shown in Fig. 3(a). The narrow width indicates the rapid disappearance of the ring-like features. With the other CEPs, the ratio is constant, and this creates a round spot with a near-flat top distribution, as shown in Fig. 3(b). The reason for this relationship between the CEP and the ratio is the rapid decrease in the local THz intensity produced away from the focus, as shown in Fig. 1(a).

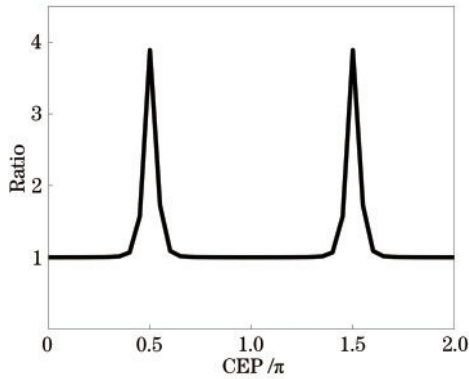


Fig. 5 Peak-to-valley ratio (< 3 THz) evolved with φ_0

Using these characteristics, we propose a scheme to measure the φ_0 of few-cycle pulses accurately. This can be achieved by changing the CEP of few-cycle pulses such that the far-field pattern becomes a ring with the highest contrast. The value of φ_0 can be 0.5π or 1.5π , depending on its polarity. The distinction between 0.5π and 1.5π can be resolved by measuring the local THz waveform before the focal point using electro-optic sampling. Furthermore, the reliability of this solution can be verified by measuring the reversal of the local THz polarity and the phase-matching angles of different frequencies for comparison with $\cos(\theta) = 1 - \Gamma/2l_d$. Compared with other methods of CEP measurement by THz emission, this scheme has a few advantages. First, it avoids the phase drift caused by the laser plasma in the filament by demanding the center CEP of 0.5π . Second, the length of the laser plasma can be flexible. The measurement error of this scheme originates from the adjustment of the CEP and THz detectors, and the deviation is estimated to be less than 100 mrad.

4 Conclusions

In conclusion, off-axis phase-matched THz emission driven by few-cycle laser pulses in a gaseous medium was investigated. We found that the amplitudes and angular distributions of the far-field THz emission are sensitive to the focal CEP. Owing to the antisymmetric THz emission before and after the focus, the far-field exhibits a ring-like pattern at 0.5π and 1.5π . When the CEP deviates from 0.5π or 1.5π , the far-field pattern rapidly loses its ring characteristics and degenerates into a circular spot distribution. Finally, we propose a scheme to determine the focal CEP accurately. This reliable and accurate focal CEP measurement scheme is valuable for regulating CEP-dependent physical phenomena.

References

- [1] Apolonski A, Poppe A, Tempea G, et al. Controlling the phase evolution of few-cycle light pulses[J]. *Physical Review Letters*, 2000, 85(4): 740-743.
- [2] Jones D J, Diddams S A, Ranka J K, et al. Carrier-envelope phase control of femtosecond mode-locked lasers and direct optical frequency synthesis[J]. *Science*, 2000, 288(5466): 635-640.
- [3] Krausz F, Ivanov M. Attosecond physics[J]. *Reviews of Modern Physics*, 2009, 81(1): 163-234.
- [4] Hollinger R, Hoff D, Wustelt P, et al. Carrier-envelope-phase measurement of few-cycle mid-infrared laser pulses using high harmonic generation in ZnO[J]. *Optics Express*, 2020, 28(5): 7314-7322.
- [5] Xiang Y, Lu J, Niu Y P, et al. Measuring the carrier-envelope phases of few-cycle laser pulses using the high-order harmonic spectrum from asymmetric molecules[J]. *Journal of Physics B: Atomic, Molecular and Optical Physics*, 2015, 48(13): 135601.
- [6] Paulus G G, Lindner F, Walther H, et al. Measurement of the phase of few-cycle laser pulses[J]. *Physical Review Letters*, 2003, 91(25): 253004.
- [7] Sayler A M, Rathje T, Müller W, et al. Precise, real-time, every-single-shot, carrier-envelope phase measurement of ultrashort laser pulses[J]. *Optics Letters*, 2011, 36(1): 1-3.
- [8] Wittmann T, Horvath B, Helml W, et al. Single-shot carrier-envelope phase measurement of few-cycle laser pulses[J]. *Nature Physics*, 2009, 5(5): 357-362.
- [9] Bai Y, Li C, Liu P, et al. Characterizing the polarity of a few-cycle infrared laser pulse[J]. *Applied Physics B*, 2012, 106(1): 45-49.
- [10] Bai Y, Song L W, Xu R J, et al. Waveform-controlled terahertz radiation from the air filament produced by few-cycle laser pulses[J]. *Physical Review Letters*, 2012, 108(25): 255004.
- [11] Wu H C, Meyer-Ter-Vehn J, Sheng Z M. Phase-sensitive terahertz emission from gas targets irradiated by few-cycle laser pulses[J]. *New Journal of Physics*, 2008, 10(4): 043001.
- [12] Xu R J, Bai Y, Song L W, et al. Initial carrier-envelope phase of few-cycle pulses determined by terahertz emission from air plasma[J]. *Applied Physics Letters*, 2013, 103(6): 061111.
- [13] Xu R J, Bai Y, Song L W, et al. Terahertz emission by balanced nonlinear effects in air plasma[J]. *Chinese Optics Letters*, 2013, 11(12): 123002.
- [14] Zhang Z L, Chen Y P, Cui S, et al. Manipulation of polarizations for broadband terahertz waves emitted from laser plasma filaments[J]. *Nature Photonics*, 2018, 12(9): 554-559.
- [15] Mackenroth F, Di Piazza A, Keitel C H. Determining the carrier-envelope phase of intense few-cycle laser pulses[J]. *Physical Review Letters*, 2010, 105(6): 063903.
- [16] Porras M A. Diffraction effects in few-cycle optical pulses

- [J]. *Physical Review E*, 2002, 65(2 Pt 2): 026606.
- [17] Kreß M, Löffler T, Thomson M D, et al. Determination of the carrier-envelope phase of few-cycle laser pulses with terahertz-emission spectroscopy[J]. *Nature Physics*, 2006, 2(5): 327-331.
- [18] Lindner F, Paulus G G, Walther H, et al. Gouy phase shift for few-cycle laser pulses[J]. *Physical Review Letters*, 2004, 92(11): 113001.
- [19] Kim K Y. Generation of coherent terahertz radiation in ultrafast laser-gas interactions[J]. *Physics of Plasmas*, 2009, 16(5): 056706.
- [20] Kim K Y, Glowia J H, Taylor A J, et al. Terahertz emission from ultrafast ionizing air in symmetry-broken laser fields[J]. *Optics Express*, 2007, 15(8): 4577-4584.
- [21] Kim K Y, Taylor A J, Glowia J H, et al. Coherent control of terahertz supercontinuum generation in ultrafast laser-gas interactions[J]. *Nature Photonics*, 2008, 2(10): 605-609.
- [22] Audebert P, Daguzan P, Dos Santos A, et al. Space-time observation of an electron gas in SiO₂[J]. *Physical Review Letters*, 1994, 73(14): 1990-1993.
- [23] Ammosov M V, Delone N B, Krainov V P. Tunnel ionization of complex atoms and atomic ions in a varying electromagnetic-field[J]. *Journal of Experimental and Theoretical Physics*, 1986, 91(6): 2008-2013.
- [24] You Y S, Oh T I, Kim K Y. Off-axis phase-matched terahertz emission from two-color laser-induced plasma filaments[J]. *Physical Review Letters*, 2012, 109(18): 183902.
- [25] Klarskov P, Strikwerda A C, Iwaszczuk K, et al. Experimental three-dimensional beam profiling and modeling of a terahertz beam generated from a two-color air plasma[J]. *New Journal of Physics*, 2013, 15(7): 075012.
- [26] Li N, Bai Y, Miao T S, et al. Revealing plasma oscillation in THz spectrum from laser plasma of molecular jet[J]. *Optics Express*, 2016, 24(20): 23009-23017.
- [27] Li X L, Bai Y, Li N, et al. Absorption of laser plasma in competition with oscillation currents for a terahertz spectrum[J]. *Optics Letters*, 2018, 43(1): 114-117.